

## PERLE – LATTICE DESIGN AND BEAM DYNAMICS STUDIES\*

S. A. Bogacz<sup>†</sup>, D. Douglas, F. Hannon, A. Hutton, F. Marhauser, R. Rimmer, Y. Roblin,  
C. Tennant, Jefferson Lab, Newport News, USA

G. Arduini, O. Brüning, R. Calaga, K-M. Schirm, F. Gerigk, B. Holzer, E. Jensen, A. Milanese,  
E. Montesinos, D. Pellegrini, P-A. Thonet, D. Schulte, A. Valloni, CERN, Geneva, Switzerland

I. Chaikovska, W. Kaabi, A. Stocchi, C. Vallerand, LAL, Orsay, France

S. Bousson, D. Longuevergne, G. Olivier, G. Olry, IPN, Orsay, France

D. Angal-Kalinin, J. McKenzie, B. Militsyn, P. Williams, STFC Daresbury Laboratory,  
Warrington, UK

B. Hounsell, M. Klein, U. Klein, P. Kostka, C. Welsch, University of Liverpool, Liverpool, UK

E. Levichev, Y. Pupkov, BINP, Novosibirsk, Russia

### Abstract

PERLE (Powerful ERL for Experiments) is a novel ERL test facility [1], which has been designed to validate choices for a 60 GeV ERL foreseen in the design of the LHeC [2] and the FCC-eh. Its main thrust is to probe high current, CW, multi-pass operation with superconducting cavities at 802 MHz (and perhaps testing other frequencies of interest). With very high transient beam power (~10 MW), PERLE offers an opportunity for controllable study of every beam dynamic effect of interest in the next generation of ERL design and become a ‘stepping stone’ between present state-of-art 1 MW ERLs and future 100 MW scale applications. PERLE design features Flexible Momentum Compaction lattice architecture for six vertically stacked return arcs and a high-current, 5 MeV, photo-injector. With only one pair of 4 cavity cryomodules, 400 MeV beam energy can be reached in 3 recirculation passes, with beam currents of about 20 mA. The beam is decelerated in 3 consecutive passes back to the injection energy, transferring the beam energy back to the RF. This unique facility will serve as a test-bed for high current ERL technologies and a user facility in low energy electron and photon physics [3]. Work has begun to evaluate system performance in the presence of collective effects and other beam dynamical processes especially relevant in a multi-pass ERL configuration.

### LAYOUT AND ENERGY

PERLE accelerator complex is arranged in a racetrack configuration; hosting two cryomodules (containing four, 5-cell, cavities operating at 802 MHz), each located in one of two parallel straights, completed with a vertical stack of three recirculating arcs on each side. The straights are about 10 meters long and the 180° arcs are 5.5 meters across. Additional space is taken by 4-meter long spreaders/recombiners, including matching sections. As illustrated in Fig. 1, the total ‘footprint’ of PERLE is: 24 m × 5.5 m × 0.8 m; the last dimension reflecting 40 cm vertical separation between the arcs. Each of the two cryomodules provides 65.5 MeV energy boost (higher gradients around 20 MV/m will also be explored). Therefore,

in three turns, a 393 MeV energy increase is achieved. Adding initial injection energy of about 5 MeV yields the total energy of 398 MeV – call it ‘400 MeV’.

### LATTICE DESIGN ARCHITECTURE

Multi-pass energy recovery in a racetrack topology, with identical linacs, explicitly requires that both the accelerating and the decelerating beams share the individual return arcs. This in turn, imposes specific requirements for the Twiss function at the linacs ends: the Twiss functions have to be identical for both the accelerating and decelerating linac passes converging to the same energy and therefore entering the same arc.

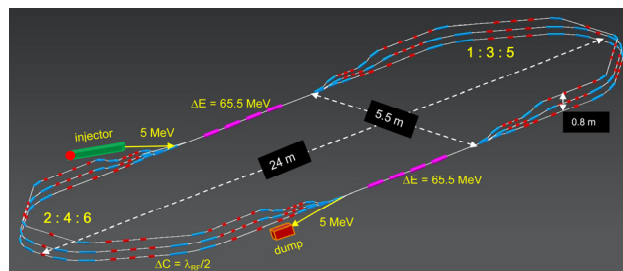


Figure 1: PERLE layout featuring two parallel linacs each hosting a 65.5 MeV cryomodule, achieving 400 MeV in three passes.

Injection at about 5 MeV into the first linac is done through a fixed field injection chicane, with its last magnet (closing the chicane) being placed at the beginning of the linac. It closes the orbit ‘bump’ at the lowest energy, injection pass, but the magnet (physically located in the linac) will deflect the beam on all subsequent linac passes. In order to close the resulting higher pass ‘bumps’, the so-called reinjection chicane is instrumented, by placing two additional opposing bends in front of the last chicane magnet. This way, the re-injection chicane magnets are only ‘visible’ by the higher pass beams.

The second linac in the racetrack is configured exactly as a mirror image of the first one, with a replica of the reinjection chicane at its end, which facilitates a fixed-field extraction of energy recovered beam to the dump.

The spreaders are placed directly after each linac to separate beams of different energies and to route them to the corresponding arcs. The recombiners facilitate just the

\* Work has been authored by Jefferson Science Associates, LLC under Contract No. DE-AC05-06OR23177 with the U.S. Dep. of Energy.

<sup>†</sup> bogacz@jlab.org

opposite: merging the beams of different energies into the same trajectory before entering the next linac. As illustrated in Fig. 2, each spreader starts with a vertical bending magnet, common for all three beams, which initiates the separation.

The highest energy, at the bottom, is brought back to the initial linac level with a chicane. The lower energies are captured with a two-step vertical beamline. The vertical dispersion introduced by the first-step bends is suppressed by the three quadrupoles located appropriately between the two steps. The lowest energy spreader is configured with three curved bends following the common magnet, because of the large bending angle ( $45^\circ$ ) of the spreader. This minimizes adverse effects of strong edge focusing on dispersion suppression for the lower energy spreader. Following the spreader, there are four matching quads to ‘bridge’ the Twiss function between the spreader and the following  $180^\circ$  arc (two betas and two alphas).

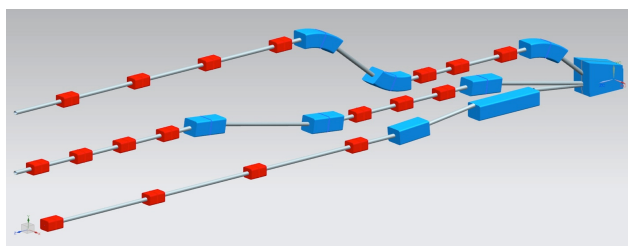


Figure 2: Layout of a three-beam switchyard with the corresponding energy ratios: 1 : 3 : 5.

All six,  $180^\circ$  horizontal arcs are configured with the FMC optics to ease individual adjustment of  $M_{56}$  in each arc (needed for the longitudinal phase-space re-shaping, essential for operation with energy recovery). The lower energy arcs (1, 2, 3) are composed of four 45.6-cm long, curved  $45^\circ$  bends and of a series of quadrupoles (two triplets and one singlet), while the higher arcs (4, 5, 6) use ‘double length’, 91.2 cm long, curved bends. The use of curved bends is dictated by the large bending angle ( $45^\circ$ ). If rectangular bends were used, their edge focusing would cause significant focusing imbalance, which in turn, would have an adverse effect on the overall arc optics. Another reason for using curved bends is to eliminate the problem of magnet sagitta, which would be especially significant for the longer 91.2-cm bends. Each arc is followed by a matching section and a recombiner (mirror symmetric to spreader and matching section). Since the linacs are mirror-symmetric, the matching conditions described in the previous section, impose mirror-symmetric arc optics (identical betas and sign reversed alphas at the arc ends). A complete lattice for arc 1 at 70.5 MeV, including a spreader,  $180^\circ$  horizontal arcs and a recombiner, is illustrated in Fig. 3. The final arc optics features a high degree of modular functionality to facilitate momentum compaction management, as well as orthogonal tunability for both the beta functions and dispersion.

The path-length of each arc is chosen to be an integer number of RF wavelengths, except for the highest energy pass, arc 6, whose length is longer by half of the RF

wavelength (to shift the RF phase from accelerating to decelerating, switching to the energy recovery mode).

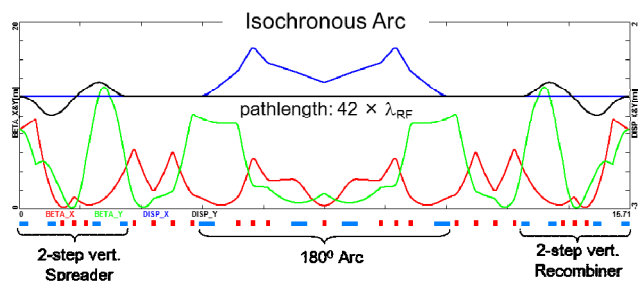


Figure 3: Optics based on the FMC cell for the lowest energy return arc. Horizontal (red) and vertical (green) beta-function amplitudes are illustrated. Blue and black curves represent the horizontal and vertical dispersion. The arc is tuned to the isochronous condition ( $M_{56} = 0$ ).

## BEAM DYNAMICS STUDIES

Given the baseline lattice described in the previous section, work has begun to evaluate system performance in the presence of collective effects and other beam dynamical processes. In particular, because PERLE utilizes multiple passes and the beam is bent through  $1080$  degrees, managing coherent synchrotron radiation (CSR) and the microbunching instability (mBI) will be crucial.

When a bunch travels along a curved orbit, fields radiated from the tail of the bunch can overtake and interact with the head. Rather than the more conventional class of head-tail instabilities where the tail is affected by the actions of the head, CSR is a tail-head instability. The net result is that the tail loses energy while the head gains energy leading to an undesirable gross distortion along the bunch. Because the interaction takes place in a region of dispersion, the energy redistribution is correlated with the transverse positions in the bend plane and can lead to growth of the projected emittance.

There has been success in recent years to undo the effects of CSR in the bend plane with an appropriate choice of beam optics [4]. Though possible to control the transverse emittance growth, it is more difficult to undo the gross longitudinal distortion caused by the CSR wake – particularly in applications where the intrinsic energy spread is small and/or where the effect can accumulate over multiple recirculations. Initial simulations for PERLE indicate that while the CSR-induced distortion is masked by the large projected energy spread of the beam at high energy, the distortion becomes evident and problematic at lower energy (e.g. during energy recovery) [5]. The longitudinal phase space is further affected by CSR due to the drop in centroid energy as power is radiated away. Initial estimates indicate several kW of power will be lost to CSR during 3-pass up/down operation. This is particularly relevant to the PERLE design where the consequent energy mismatch must be managed to allow lossless transmission through common transport. One possible mitigation scheme is shielding of the CSR wake from

the beam pipe. Care must be taken however, so as to not aggravate beam loss from halo.

Additionally, CSR can drive the microbunching instability. The mechanism by which microbunching develops is as follows: an initial density modulation, either from shot noise or from the drive laser, is converted to energy modulations through short-range wake-fields such as space charge and CSR. The energy modulations are then transformed back to density modulations through the momentum compaction of the lattice. Danger arises when a positive feedback is formed and the initial modulations are enhanced. This phenomenon has been studied extensively, both theoretically and experimentally, in bunch compressor chicanes. Only recently has there been a concerted effort to study the microbunching instability in recirculating arcs [6, 7]. Energy recovery linacs can be particularly susceptible to microbunching. For increased efficiency, ERLs inject beam at low energy and the beam is influenced by space charge forces. Due to the topology required in same-cell energy recovery, ERLs necessarily have substantial bending and are subject to the effects of CSR. And – unlike space charge – the effects of CSR do not diminish at high energy. Because the beam is subject to space charge and/or CSR throughout the machine, density modulations can be converted to energy modulations. And because of the native momentum compaction of the lattice (in arcs, spreaders/recombiners, chicanes, etc.) those energy modulations may be converted back to density modulations. Therefore, in ERLs with high brightness beams, conditions are favorable for seeding the microbunching instability.

Studying the microbunching instability in the time-domain (i.e. via particle tracking) presents multiple challenges. The initial density modulation needs to be small enough to remain in the linear regime but large enough to overcome numerical artifacts, which requires a large number of particles. Due to the computational burden, it becomes difficult to exercise parametric studies and/or model an entire accelerator complex. On the other hand, a semi-analytical Vlasov solver that works in the frequency-domain and models relevant collective effects such as longitudinal space charge, CSR and linac geometric effects using analytic impedance expressions allows for quick analysis, even for large systems [8]. Using the Vlasov-solver to compute the microbunching gain curve for the first recirculation in PERLE gives the result shown in Fig. 4. The peak occurs at a wavelength of about 750 microns with a gain of 16. In multi-pass systems, the total gain goes roughly as the gain for a single pass raised to the number of passes. Therefore, absent any changes in the lattice or beam parameters (simulations assumed an rms intrinsic energy spread of 10 keV), microbunching will be a serious issue. This is not entirely surprising given that MESA, a similar 3-pass up/down ERL design at the University of Mainz, faces a similar issue with microbunching [9].

In addition to CSR and mBI, another relevant effect in ERLs is multi-pass beam breakup (BBU), which occurs when the electron beam interacts with the higher-order

modes (HOMs) of an accelerating cavity on the accelerating pass and again on the energy recovered pass. Above a certain threshold current, the beam goes unstable and is lost. The instability is well understood and has a solid theoretical and experimental foundation [10, 11]. However, much of the experimental work was on a 1-pass up/down machine whereas PERLE – with its multiple recirculations – presents a unique testbed for understanding how BBU scales with the number of passes.

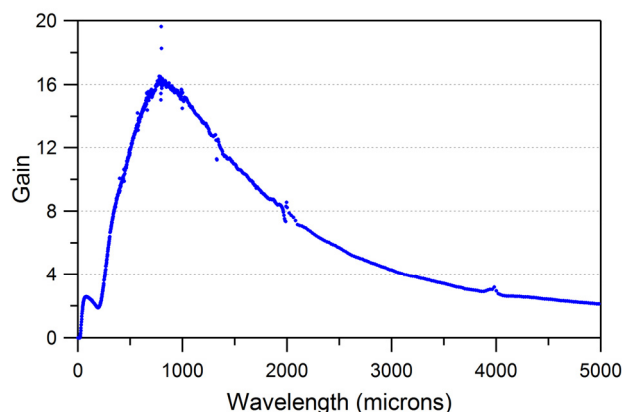


Figure 4: mBI gain for the first recirculation in PERLE.

One of the most difficult operational challenges for ERLs is halo – and specifically beam loss generated by halo [12]. Scattering, nonlinear effects in both beam and lattice, and collective effects within the beam and due to beam interactions with its environment drive halo formation, which is a critical challenge as ERL virtual beam power increases. This concern is based on the reality that ERLs are non-equilibrium systems. That is to say, beams are not only non-Gaussian, they exhibit complex structure and thus have halo components that both sample very large amplitudes and carry sufficient power to damage beamline elements [13]. To adequately assess the impact of halo requires simulating realistic particle distributions with a very large numbers of particles. Processes that may generate halo particles include intra-beam, Touschek and beam/gas scattering – all mechanisms whose impact must be assessed (and perhaps collimated).

## SUMMARY – OUTLOOK

A half-century of testing and application of ERL-based systems has resulted in considerable progress with energy-recovery technology, but numerous questions still remain. Next-generation systems thus have excellent opportunities to explore basic beam dynamical issues and resolve engineering challenges. PERLE combines beam energy, current, power, brightness, and operational flexibility in a combination unavailable in any other existing or proposed ERL, e.g. validation of HOM/power couplers and LLRF systems, as well as identification of required beam instrumentation for future high-energy, high-current, multi-turn ERLs. It can therefore support testing throughout an unmatched region of parameter space, informing and providing the required technology base for the design of future generations of accelerators, including

high-energy colliders (the LHeC and FCC-eh, in particular), non-equilibrium systems for electron cooling, and high-power/short-wavelength FEL drivers, e.g. the UKXFEL [14, 15].

## REFERENCES

- [1] G. Arduini *et al.*, "PERLE: Powerful ERL for Experiments – Conceptual Design Report", *Journal of Physics G*, 2007, doi:org/10.1088/1361-6471/aaa171
- [2] D. Pellegrini, A. Latina, D. Schulte, and S.A. Bogacz, "Beam-dynamics Driven Design of the LHeC Energy Recovery Linac", *Phys. Rev. ST Accel. Beams*, vol. 18, p. 121004, Dec. 2015, doi:10.1103/PhysRevSTAB.18.121004
- [3] E. Jensen *et al.*, "PERLE - a Powerful ERL Facility Concept", in *Proc. Nucl. Photonics Conf.*, Monterey, CA, to be published.
- [4] S. DiMitri, M. Cornacchia, and S. Spampinati, "Cancellation of Coherent Synchrotron Radiation Kicks with Optics Balance", *Phys. Rev. Lett.*, vol. 110, p. 014801, 2013, doi:10.1103/PhysRevLett.110.014801
- [5] D. Douglas, "CSR Estimates for PERLE", Jefferson Laboratory, Newport News, VA 23606, U.S.A., Technical Note 17-014, 2017.
- [6] S. DiMitri and M. Cornacchia, "Transverse Emittance-preserving Arc Compressor for High-brightness Electron Beam-based Light Sources and Colliders", *Eur. Phys. Lett.*, vol. 109, p. 62002, 2015, doi:10.1209/0295-5075/109/62002
- [7] C.-Y. Tsai, S. DiMitri, D. Douglas, R. Li, and C. Tennant, "Conditions for Coherent-synchrotron-radiation-induced Microbunching Suppression in Multibend Beam Transport or Recirculation Arcs", *Phys. Rev. Accel. Beams*, vol. 20, p. 024401, 2017, doi:10.1103/PhysRevAccelBeams.20.024401
- [8] C.-Y. Tsai, D. Douglas, R. Li, and C. Tennant, "Linear Microbunching Analysis for Recirculation Machines", *Phys. Rev. Accel. Beams*, vol. 19, p. 114401, 2016, doi:10.1103/PhysRevAccelBeams.19.114401
- [9] A. Khan, "Study of Microbunching Instability in MESA", in *59th ICFA Advanced Beam Dynamics Workshop on Energy Recovery Linacs (ERL'17)*, CERN, Switzerland, to be published.
- [10] C. Tennant *et al.*, "First Observations and Suppression of Multipass, Multibunch Beam Breakup in the Jefferson Laboratory Free Electron Laser Upgrade", *Phys. Rev. Accel. Beams*, vol. 8, p. 074403, 2005, doi:10.1103/PhysRevSTAB.8.074403
- [11] D. Douglas, *et al.*, "Experimental Investigation of Multi-bunch, Multipass Beam Breakup in the Jefferson Laboratory Free Electron Laser Upgrade Driver", *Phys. Rev. Accel. Beams*, vol. 9, p. 064403, 2006, doi:10.1103/PhysRevSTAB.9.064403
- [12] O. Tanaka, "New Halo Formation Mechanism at the KEK Compact Energy Recovery Linac", *Phys. Rev. Accel. Beams*, vol. 21, p. 024202, 2018, doi:10.1103/PhysRevAccelBeams.21.024202
- [13] D. Douglas, *et al.*, "Why PERLE?", Jefferson Laboratory, Newport News, VA 23606, U.S.A., Technical Note 18-000, 2018.
- [14] P. Williams, *et al.*, "A Staged, Multi-User X-Ray Free Electron Laser & Nuclear Physics Facility Based on a Multi-Pass Recirculating Superconducting CW Linac", presented at FLS'18, Shanghai, P.R.China, Mar. 2018, paper THA1WA04.
- [15] N. Thompson, *et al.*, "Free-Electron Laser R&D in the UK – steps towards a national X-FEL facility", presented at FLS'18, Shanghai, P.R.China, Mar. 2018, paper TUP1WA03.